Off-Design Flow Measurements in a Centrifugal Compressor Vaneless Diffuser

A. Pinarbasi
Department of Mechanical Engineering,
University of Cumhuriyet,
Sivas, Turkey

M. W. Johnson
Department of Mechanical Engineering,
University of Liverpool,
Liverpool, United Kingdom

Detailed measurements have been taken of the three-dimensional velocity field within the vaneless diffuser of a backswept low speed centrifugal compressor using hot-wire anemometry. A 16 percent below and an 11 percent above design flow rate were used in the present study. Results at both flow rates show how the blade wake mixes out more rapidly than the passage wake. Strong secondary flows inherited from the impeller at the higher flow rate delay the mixing out of the circumferential velocity variations, but at both flow rates these circumferential variations are negligible at the last measurement station. The measured tangential/radial flow angle is used to recommend optimum values for the vaneless space and vane angle for design of a vaned diffuser.

Introduction

The performance of centrifugal compressor diffusers is highly dependent on the flow delivered from the impeller. Measurements from, for example, Krain (1988) and Farge and Johnson (1992) demonstrate that this flow is highly nonuniform and exhibits strong secondary flows. Distinct jet and wake flow regions are observed with the wake on the shroud and the jet near the hub. A strong passage vortex exists that originates in the impeller due to secondary flows. In the diffuser the impeller blade wakes are added to this already complex three-dimensional flow.

The development of these complex flows in vaneless diffusers has been studied by, for example, Inoue and Cumpsty (1984), Mizuki et al. (1985), and Senoo and Ishida (1975). Theoretically the inclusion of vanes within the diffuser should vastly improve pressure recovery, but in practice a significant improvement is only achieved over a limited flow range. This is largely because of the difficulty in achieving sensible vane incidence angles over even a small flow range. The objective of the current study on a vaneless diffuser is to obtain detailed measurements of the flow from which optimum vaneless space and vane geometry can be established for the design of a vaned diffuser. Pinarbasi and Johnson (1994) presented results for the design flow rate for the current impeller and diffuser geometry, whereas the present paper is concerned with off-design conditions.

Experimental Procedure

A schematic of the low-speed centrifugal compressor rig used in the study is shown in Fig. 1. The impeller was a De Havilland Ghost impeller, the geometry of which is given by Johnson and Moore (1980). In order to bring the geometry of this old impeller closer to that of a modern backswept impeller for the current study, the original radial outlet section was replaced to provide a 30 deg backswept outlet angle as shown in Fig. 2. The vaneless diffuser has straight walls and a constant cross-sectional area. The geometry operating conditions and measurement stations are summarized in Table 1.

Three operating points were used in the study. The "design" flow rate of $\dot{m} = 0.1311$ kg/s reported by Pinarbasi and Johnson (1994) corresponded to approximately zero incidence at the impeller blade leading edge. The "below" and "above" design flow rates of 0.1103 kg/s and 0.1450 kg/s were 16 percent below and 11 percent above the design flow rate. Detailed flow measurements within the impeller for similar flow rates are reported by Farge and Johnson (1990, 1992).

Instrumentation and Measurement Technique. A triple hot-wire probe was used to measure the velocities within the diffuser. A single wire (Dantec 55P11) was aligned circumferentially with a double wire (Dantec 55P61) arranged with each wire in the axial radial plane and at 45 deg to both the radial and axial directions. This mutually perpendicular arrangement of wires was therefore capable of resolving the axial, circumferential, and radial velocity components and the directional sign of the axial component. It was assumed that the radial and circumferential components remained positive throughout the flow. There was no evidence in the results of either of these components reducing to zero and hence this assumption was justified.

The hot wires were connected to three constant-temperature anemometer bridges. The wires were then calibrated in two stages in a wind tunnel following the procedure of Jongensen (1971). In the first stage, the velocity/voltage relationship was established with the wire perpendicular to the flow direction. King's law

$$E^2 = A + B \cdot U_e^c \tag{1}$$

was then fitted to the data for each wire using a least rms error technique to establish the calibration coefficients A, B, and C. The second stage of calibration was achieved by varying the wire orientation at fixed wind tunnel velocity to establish the directional coefficients K and H, where

$$U_e^2 = U_n^2 + K \cdot U_t^2 + H \cdot U_b^2 \tag{2}$$

U_n, U_t, and U_b are the normal, tangential, and binormal velocity components relative to the wire. K and H are also obtained by a least rms error curve fitting procedure.

An optical shaft encoder provided a pulse for every $\frac{1}{3}$ deg of impeller rotation. This was used to trigger the simultaneous sampling of the three anemometer voltages through a Microlink data acquisition unit. Readings from 57 measurement points spanning one of the 19 impeller passages were logged on each of 230 consecutive impeller revolutions. The triple wire sensor was traversed in the axial direction in order to provide a mesh of data points for each measurement plane.

Contributed by the International Gas Turbine Institute and presented at the 39th International Gas Turbine and Aeroengine Congress and Exposition, The Hague, The Netherlands, June 13–16, 1994. Manuscript received by the International Gas Turbine Institute February 4, 1994. Paper No. 94-GT-42. Associate Technical Editor: E. M. Greitzer.

Copyright © 1995 by ASME

Downloaded 08 Mar 2011 to 193.140.144.9. Redistribution subject to ASME license or copyright; see http://www.asme.org/terms/Terms_Use.cfm

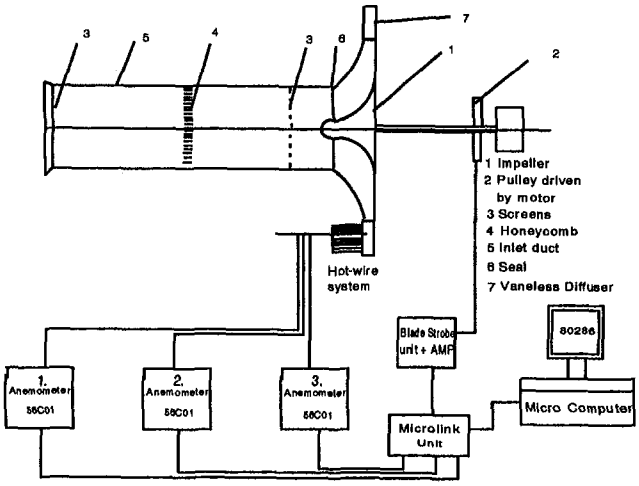


Fig. 1 Schematic of centrifugal compressor test rig

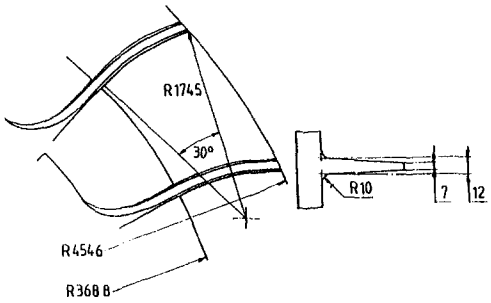


Fig. 2 Backswept impeller blade geometry

Analysis of Results. The 230 readings obtained at each measurement point for each of the three anemometers were used to compute the mean tangential, radial, and axial velocity components using the calibration coefficients. The flow rate was also computed by numerical integration of the radial velocity component over each of the measurement planes. The maximum deviation of this flow rate from the mean for all stations was 6.5 percent, which gives an indication of the overall experimental accuracy.

Mean Velocity Results

The mean velocities on the eight measurement planes in the diffuser are presented in Figs. 3–14. The radial velocity component is presented as a contour and the remaining velocity component in the measurement plane is shown as an arrow.

Station 1. The velocity distributions measured at the above and below design flow rates are shown in Figs. 3 and 4. These flow patterns are very similar to those discussed by Farge and Johnson (1992) at the impeller exit. At the above design flow rate, a very distinct passage wake is observed on the shroud at $y/y_o = 0.3$. A very strong velocity shear gradient separates this

Table 1 Geometry, operating condition, and measurement locations

Impeller Geometry and Operating Condition:

Inlet blade radius at the hub	R_h = 88.75 mm
Inlet blade radius at the shroud	R_s = 283.75 mm
Outlet radius	R_o = 454.6 mm
Backswept blade angle	$\beta = 30°$
Number of the blades	N = 19
Outlet blade span	b = 72.3 mm
Rotating speed	n = 500 rpm

Measurement Locations:

Sta.	1	2	3	4	5	6	7	8
L/R_o	0.02	0.08	0.15	0.21	0.27	0.33	0.39	0.45

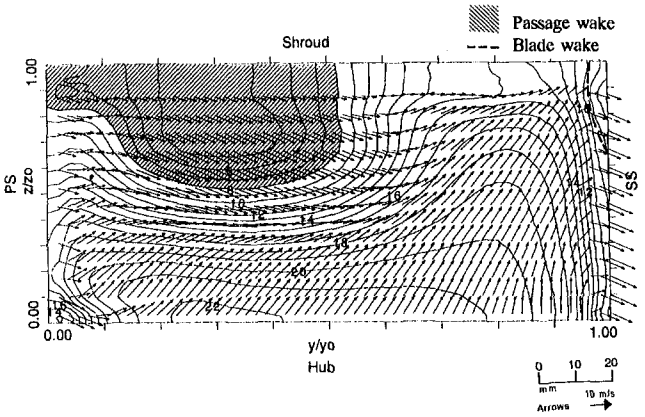


Fig. 3 Above design flow, velocities at station 1 (L/R_o = 0.02)

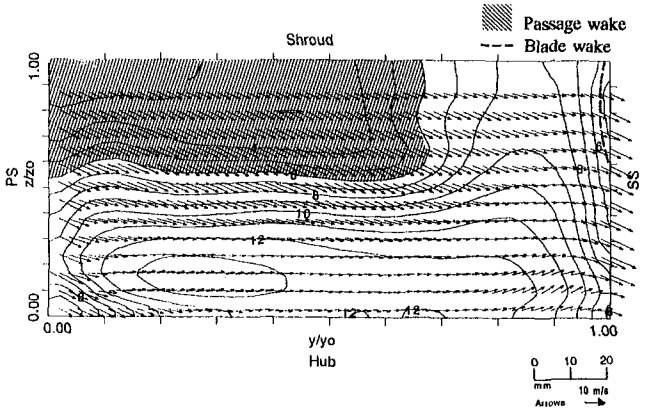


Fig. 4 Below design flow, velocities at station 1 (L/R_o = 0.02)

Nomenclature

A, B, C = King's law calibration coefficients
E = hot-wire anemometer voltage
H, K = directional coefficients for hot wire
L = radial distance from impeller outlet
R_o = impeller outlet radius
U_e = effective cooling velocity
U_r, U_θ, U_z = radial, tangential, and axial velocity components
y = tangential coordinate in measurement plane
y_o = tangential distance between consecutive blade wakes
z = axial coordinate in measurement plane
z_o = axial diffuser width in measurement plane

Downloaded 08 Mar 2011 to 193.140.144.9. Redistribution subject to ASME license or copyright; see http://www.asme.org/terms/Terms_Use.cfm

region from the rest of the flow. The blade wake is observed on the suction side between $y/y_o = 0.95$ and 1. Strong secondary velocities sweep high-velocity fluid from the hub to the shroud near the suction side and low-energy fluid from the blade and passage wakes in the shroud-to-hub direction. The large difference in flow angle between the blade wake and adjacent passage flow led to rapid mixing out of the blade wake at the design flow rate (Pinarbasi and Johnson, 1994).

For the below design flow rate (Fig. 4), the passage wake, jet, and blade wake are less distinct. The location of the passage wake is similar, but the wake is larger and is spread over a much larger proportion of the shroud. The secondary flows are also weaker, particularly the flow up the suction side; however, there is still evidence of opposed secondary flows on either side of the blade wake.

Station 2. Figure 5 shows that the secondary flows are still strong for the above design flow rate at station 2. The rapid variation in flow angle across the blade wake has indeed largely resulted in the mixing out of the blade wake observed at $y/y_o = 0.1$. This is in fact the blade wake from the neighboring passage, which has been convected to its current location by the tangential velocity component. The passage wake has moved more rapidly in this direction, because of its lower radial velocity and hence larger flow angle. The wake has altered shape and has spread over the shroud. It has altered little in size and hence the mixing mechanisms within this region are clearly much weaker than those in the blade wake region.

At the below design flow rate (Fig. 6), the blade wake has been convected further than for the higher flow rate to $y/y_o \approx 0.15$, but again has substantially mixed out. The passage wake has been convected to $y/y_o \approx 0.4$, but has altered little in size. There are now only small variations of secondary velocity in the circumferential direction at this flow rate.

Station 3. The passage wake has continued to move and spread across the shroud between stations 2 and 3 for the above design flow rate (Fig. 7). It has, however, continued to traverse faster than the blade wake, which is still just discernable near the hub. Relatively strong secondary flows are still observed in Fig. 7 with marked variations in the circumferential direction. However, the variations in radial velocity in this direction have now decreased significantly from station 1 with the velocity contours aligned parallel with the diffuser walls.

Mixing out in the circumferential direction is almost complete for the below design flow (Fig. 8) and there is also some evidence of thickening of the hub boundary layer as the peak velocity in the jet region has been displaced toward the center of the passage. The passage wake has now spread almost evenly along the shroud wall. The main variation in radial velocity in the circumferential direction is associated with the blade wake, which is skewed across the passage. This skewing is due to the more rapid translation in the circumferential direction of the low-energy fluid near the hub and shroud walls as compared with the high-energy fluid in the jet.

Station 4. At station 4 for the above design flow rate (see Fig. 9) the passage wake occupies most of the shroud surface. The blade wake is still detected near the hub. There is now some evidence of thickening of the hub boundary layer from the displacement of the jet peak velocity region from the hub wall to $z/z_o \approx 0.1$. The strong axial velocity component near the hub walls is also an indication of diffusion as the jet slows from 22 m/s at station 1 to 17 m/s at the current station.

The below design flow (Fig. 10) now closely resembles a Couette flow between the diffuser walls, although the hub boundary layer is still much thinner than that on the shroud, which is reflected in the off-center position of the peak velocity at $z/z_o = 0.3$.

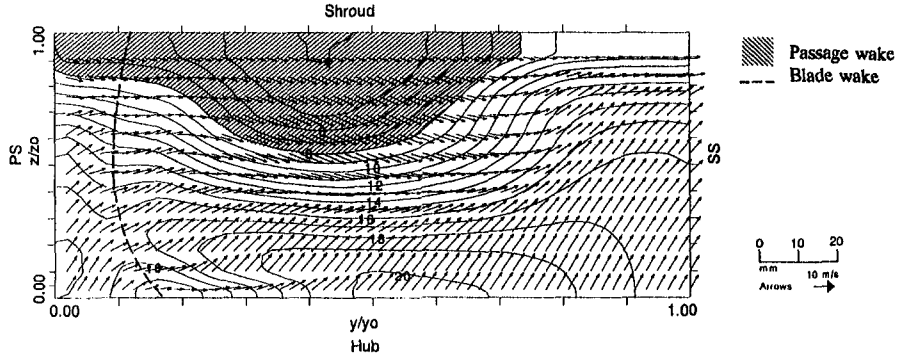


Fig. 5 Above design flow, velocities at station 2 ($L/R_o = 0.08$)

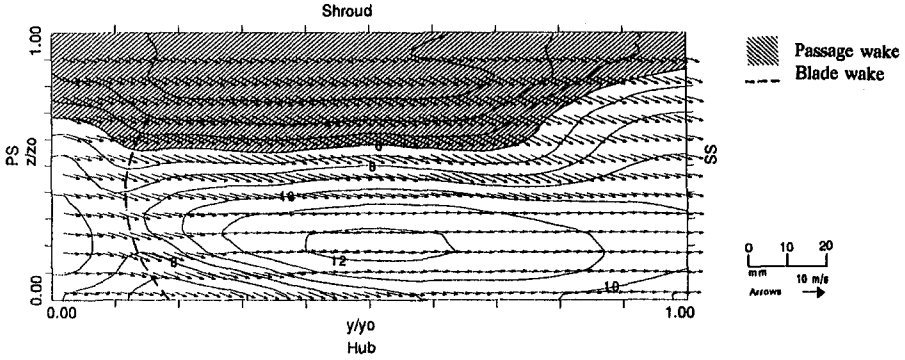


Fig. 6 Below design flow, velocities at station 2 ($L/R_o = 0.08$)

Downloaded 08 Mar 2011 to 193.140.144.9. Redistribution subject to ASME license or copyright; see http://www.asme.org/terms/Terms_Use.cfm

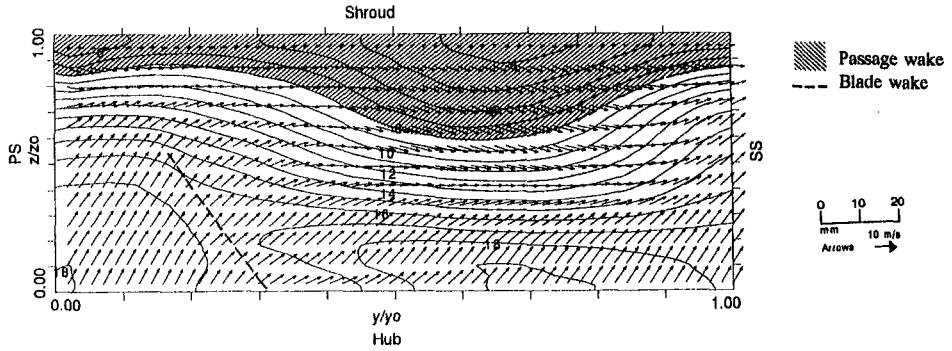


Fig. 7 Above design flow, velocities at station 3 (L/R_o = 0.15)

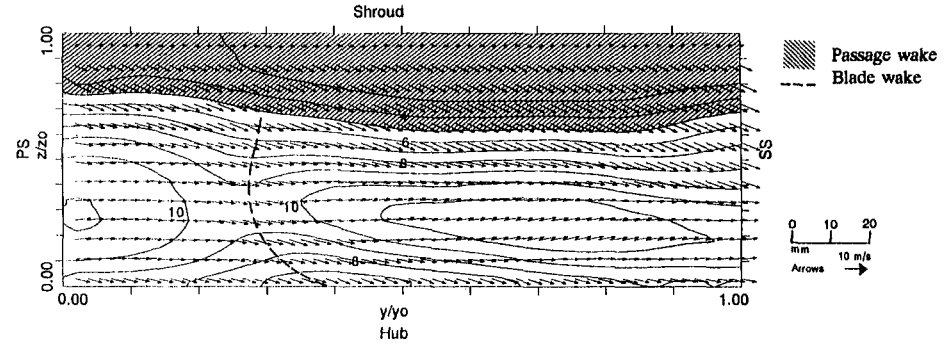


Fig. 8 Below design flow, velocities at station 3 (L/R_o = 0.15)

Stations 5 to 8. As the flow progresses through the diffuser, it continues to tend toward a Couette flow. This process is more advanced in the case of the below design flow as shown by Figs. 12 (Station 6) and 14 (Station 8) than for the above design flow case at the same stations (see Figs. 11 and 13). Figure 14 shows that at the last station for the below design flow, the peak velocity region is at z/z_o = 0.35, and the hub boundary layer is still two to three times thinner than its shroud counterpart. In contrast, for the above design flow rate (Fig. 13), the peak velocity region is still very close to the hub wall

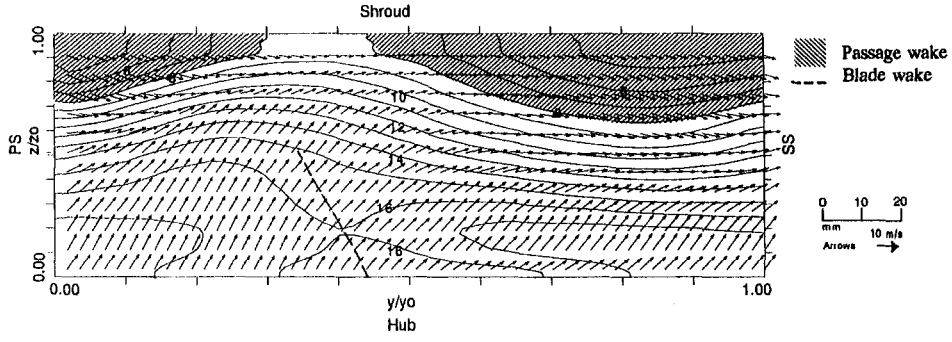


Fig. 9 Above design flow, velocities at station 4 (L/R_o = 0.21)

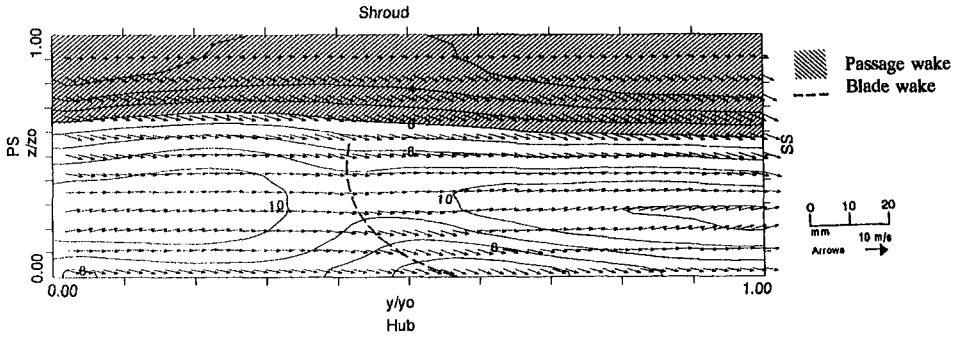


Fig. 10 Below design flow, velocities at station 4 (L/R_o = 0.21)

Downloaded 08 Mar 2011 to 193.140.144.9. Redistribution subject to ASME license or copyright; see http://www.asme.org/terms/Terms_Use.cfm

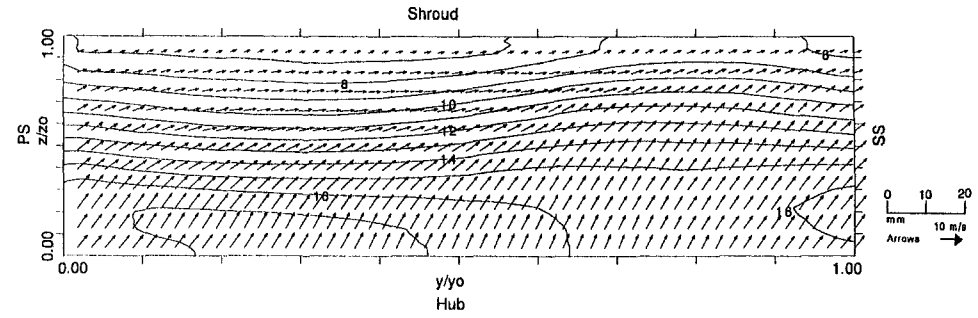


Fig. 11 Above design flow, velocities at station 6 (L/R_o = 0.33)

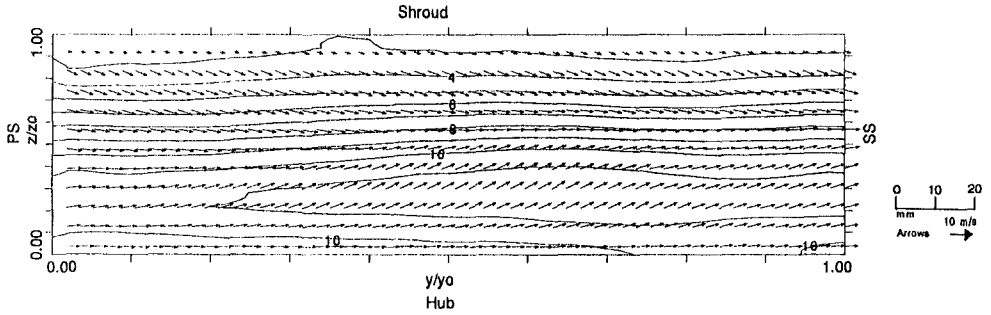


Fig. 12 Below design flow, velocities at station 6 (L/R_o = 0.33)

(z/z_o = 0.1) and the hub boundary layer thickness is perhaps only 10 percent of that on the shroud. The reason for this difference is believed to be the stronger secondary flows observed at the higher flow rate up to station 3, which continue to extract low-energy fluid from the hub boundary layer and hence re-energize it.

Flow Angle Results

Station 1. Figures 15 and 16 show the differences between the flow angle ($\tan^{-1}(U_\theta/U_r)$) for the two flow rates at the diffuser inlet.

At the above design flow rate (Fig. 15) the flow angle variation is extreme with angles as high as 75 deg in the slow moving wake and as low as 10 deg in the rapidly moving jet. For the designer of a vaned diffuser, the axial variation in flow angle can be accommodated by the use of a twisted blade. Large variations in the circumferential direction, however, will inevitably lead to significant incidence angles. It seems likely that in the current unsteady flow higher transient incidence angles may be tolerated without separation than would be the case in a steady flow. However, the magnitude of the incidence angles will still be a good guide to the likelihood of incuring significant separation losses. Figure 15 shows that the circumferential vari-

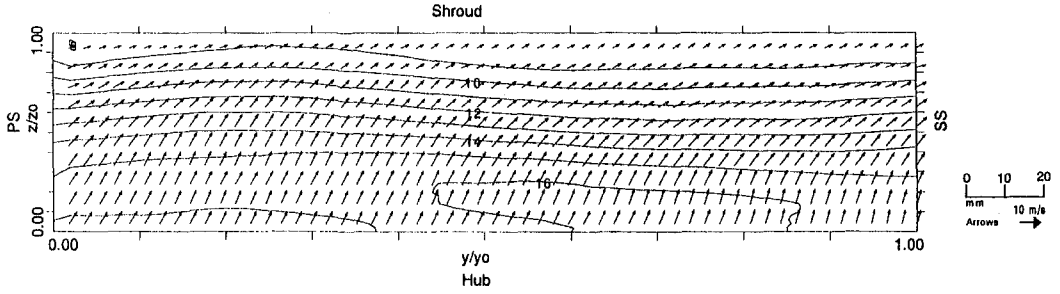


Fig. 13 Above design flow, velocities at station 8 (L/R_o = 0.45)

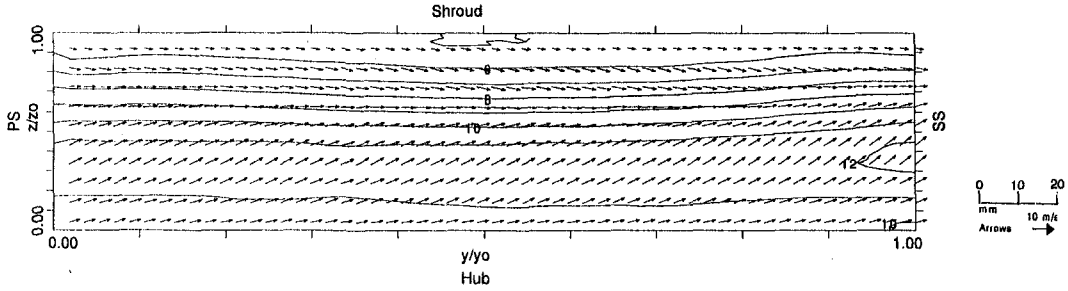


Fig. 14 Below design flow, velocities at station 8 (L/R_o = 0.45)

Downloaded 08 Mar 2011 to 193.140.144.9. Redistribution subject to ASME license or copyright; see http://www.asme.org/terms/Terms_Use.cfm

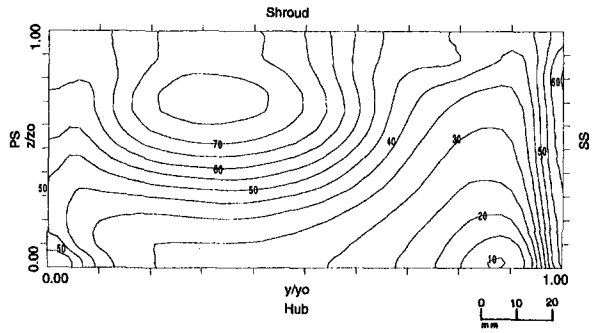


Fig. 15 Above design flow, U_θ/U_r flow angle station 1

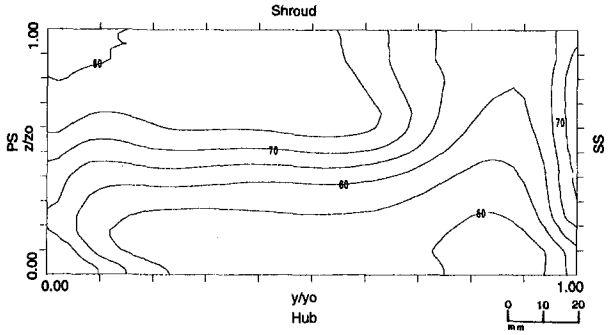


Fig. 16 Below design flow, U_θ/U_r flow angle station 1

ation in flow angle is 30 to 35 deg, which implies, for a correctly set blade, incidence angles of at least ±15 deg will result.

For the below design flow rate (Fig. 16), the flow angle variations are more modest from 50 to 80 deg with only a 15 deg circumferential variation in flow angle. A diffuser vane twisted from around 70 deg at the shroud to around 55 deg at the hub would accept this flow with a maximum incidence variation of ±8 deg where it would be expected that significant separation losses would be avoided.

Station 2. The variation in flow angle for the above design flow rate has moderated considerably at station 2 (Fig. 17) with a circumferential variation of around 20 deg. This would still lead to vane incidence angles of around ±10 deg which could induce significant separation losses.

At the below design flowrate (Fig. 18), the circumferential variation near the shroud is still about 15 deg, but is less than 10 deg closer to the hub.

Station 3. At station 3 for the above design flow rate (Fig. 19), the circumferential variation in flow angle of less than 15 deg is sufficiently low to prevent significant separation losses from a diffuser vane. The circumferential flow angle variation for the below design flow rate (Fig. 20) is now only 5 to 10 deg.

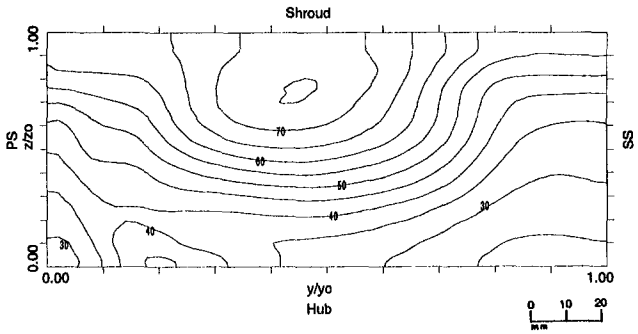


Fig. 17 Above design flow, U_θ/U_r flow angle station 2

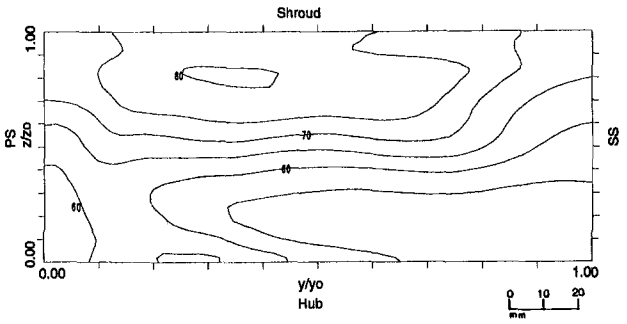


Fig. 18 Below design flow, U_θ/U_r flow angle station 2

Vaned Diffuser Design

The results of this study suggest that when designing a vaned diffuser, a vaneless space extending to $L/R_o = 0.02$ would give good performance at below design flow rates with a blade twisted from about 70 deg at the shroud to 55 deg at the hub. However, a much longer vaneless space is required at above design flow rates where $L/R_o = 0.15$ is more appropriate and the blade should be twisted from around 60 deg near the shroud to 30 deg near the hub.

If a wide range of operation is required between the flow rates considered in the current study and fixed vanes are used in the diffuser, separation losses are inevitable because of the dependence of flow angle, particularly in the jet region, on flow rate as shown by Figs. 19 and 20. However, if a vaneless space extending to station 3 ($L/R_o = 0.15$) is used, a blade twisted from around 65 deg at the shroud to about 45 deg at the hub should limit the incidence angles to ±15 deg and minimize the separation losses.

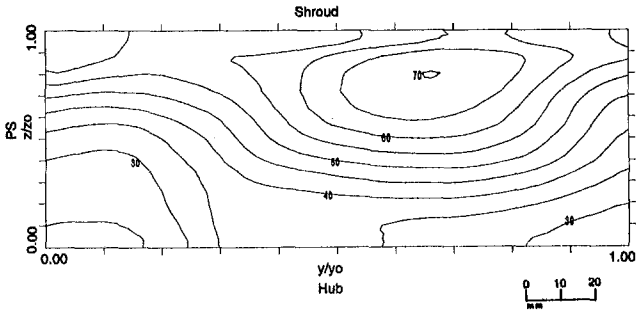


Fig. 19 Above design flow, U_θ/U_r flow angle station 3

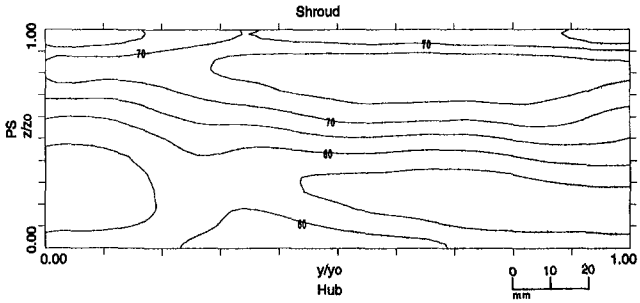


Fig. 20 Below design flow, U_θ/U_r flow angle station 3

Downloaded 08 Mar 2011 to 193.140.144.9. Redistribution subject to ASME license or copyright; see http://www.asme.org/terms/Terms_Use.cfm

Conclusions

1 The blade wake mixes out very much more rapidly than the passage wake within the vaneless diffuser.
2 At the above design flow rate the shear gradients associated with the blade and passage wakes and the secondary flows are much stronger.
3 Circumferential variations in velocity are prevented from mixing out rapidly at the higher flow rate due to the presence of the strong secondary flows.
4 The hub boundary layer is thinner than that on the shroud at the last measurement station. The ratio of the boundary layer thicknesses is around 2:1 for the below and 10:1 for the above design flow rate.
5 The optimum vaneless space for a vaned diffuser increases with flow rate, because of the slower mixing out of circumferential variations. Twisted vanes will also minimize incidence losses.
6 It is impossible to avoid significant incidence losses with fixed vane diffusers if a wide flow range is required, because of the inherent dependence of flow angle on flow rate.

References

Farge, T. Z., and Johnson, M. W., 1990, "The Effect of Backswept Blading on the Flow in a Centrifugal Compressor Impeller," ASME Paper No. 90-GT-231.

Farge, T. Z., and Johnson, M. W., 1992, "Effect of Flow Rate on Loss Mechanisms in a Backswept Centrifugal Impeller," *Int. J. Heat Fluid Flow,* Vol. 13, No. 2, pp. 189–196.

Inoue, M., and Cumpsty, N. A., 1984, "Experimental Study of Centrifugal Impeller Discharge Flow in Vaneless and Vaned Diffuser," ASME *Journal of Engineering for Gas Turbines and Power,* Vol. 106, pp. 455–467.

Johnson, M. W., and Moore, J., 1980, "The Development of Wake Flow in a Centrifugal Compressor," ASME *Journal of Engineering for Power,* Vol. 102, pp. 383–390.

Jongensen, F. E., 1971, "Directional Sensitivity of Wire and Fiber Film Probes," DISA information No. 11, pp. 31–37.

Krain, H., 1988, "Swirling Impeller Flow," ASME JOURNAL OF TURBOMACHINERY, Vol. 110, pp. 122–128.

Mizuki, S., Park, C. W., and Deckker, B., 1985, "Unstable Flows in Vaneless Diffuser of a Centrifugal Compressor at Low Flow Rates," ASME Paper No. 85-IGT-7.

Pinarbasi, A., and Johnson, M. W., 1994, "Detailed Flow Measurements in a Centrifugal Compressor Vaneless Diffuser," ASME JOURNAL OF TURBOMACHINERY, Vol. 116, pp. 453–461.

Senoo, Y., and Ishida, M., 1975, "Behavior of Severely Axymmetric Flow in a Vaneless Diffuser," ASME *Journal of Engineering for Power,* Vol. 97, pp. 375–387.

DISCUSSION

N. A. Cumpsty[1]

I am concerned that some of the measurements in this paper are inaccurate enough to be misleading. My concern centers on the velocity vectors, shown as arrows, in some of the measuring planes. When the arrows spring from a position near a solid surface, but are inclined at a large angle to the surface, there is reason to feel that something may be wrong. This is the case near the hub wall in Figs. 3, 5, 7, 9, 11, and 13, each at a progressively greater distance from the impeller outlet. The odd-numbered figures are for flow rate greater than the design value. (The corresponding even-numbered figures, at a flow rate below that for design, do not show the arrows inclined at large angles to the wall.) I am inclined to think that the measurements at the higher flow rate were compromised in some way. Would the authors care to clarify this for us?

If the measurements represented by the arrows are inaccurate, what about the velocities represented by the contours?

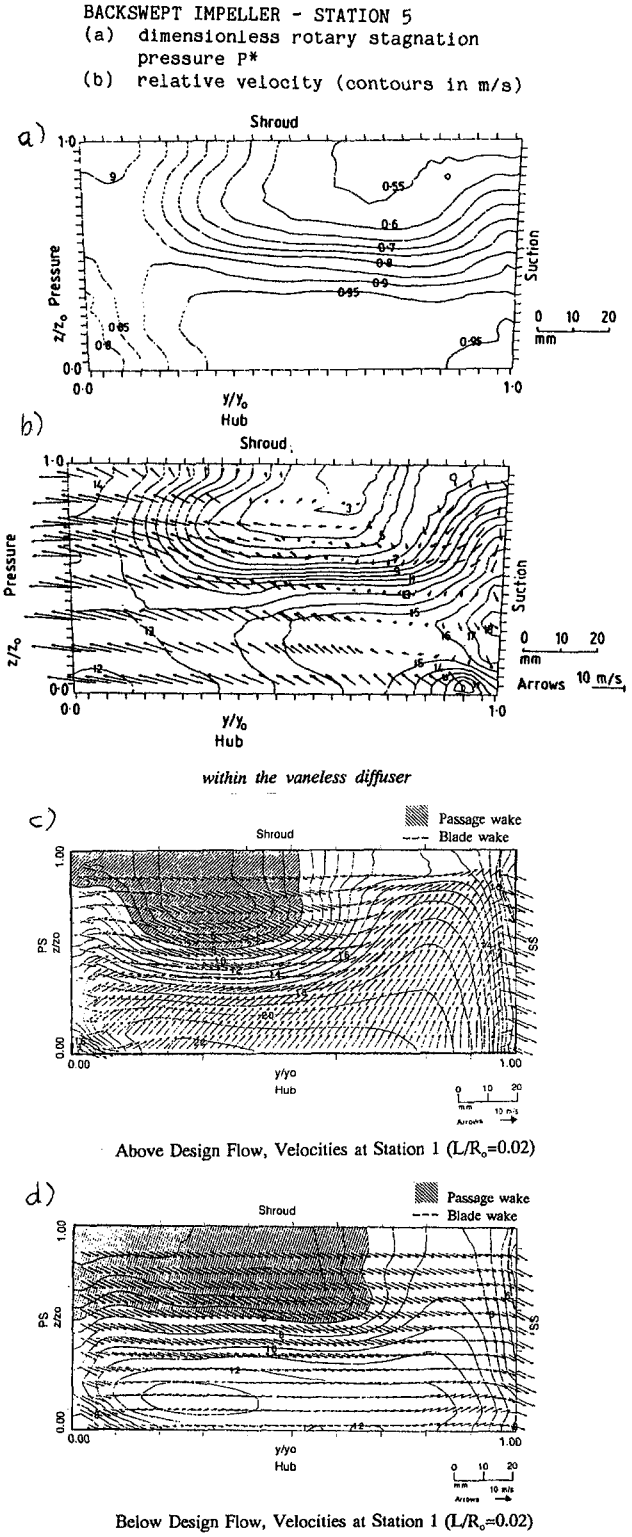


Fig. 21 Comparison of the secondary flow fields between the impeller outlet (in (*b*) at normal operating point with the corresponding dimensionless rotary stagnation pressure *p* in (*a*)), and the diffuser inlet (in (*c*) for high off-design flow at 111 percent and in (*d*) for low off-design flow at 84 percent

[1] Whittle Laboratory, Cambridge University Engineering Department, Madingley Rd., Cambridge CB3 0DY United Kingdom.

Downloaded 08 Mar 2011 to 193.140.144.9. Redistribution subject to ASME license or copyright; see http://www.asme.org/terms/Terms_Use.cfm